ELSEVIER

Synthetic Metals 135–136 (2003) 87–89

SYNTHETIC METALS

www.elsevier.com/locate/synmet

Electronic Spin-Driven Resistance in Organic-Based Magnetic Semiconductor $V[TCNE]_x$ †

V.N. Prigodin [a], N.P. Raju [a], K.I. Pokhodnya [a, b], J.S. Miller [b], and A.J. Epstein [a, c] *

[a] *Department of Physics, The Ohio State University, Columbus, Ohio 43210-1106*
[b] *Department of Chemistry, University of Utah, Salt Lake City, Utah 84112-0850*
[c] *Department of Chemistry, The Ohio State University, Columbus, Ohio 43210-1106*

Abstract

Vanadium-tetracyanoethylene ($V[TCNE]_x$, x~2) is the first organic-based magnetic semiconductor. It has the Curie temperature up to ~ 125° C and room temperature resistivity ρ_{RT} ~ 10^4 Ωcm. Here we present the first observation of an increase in resistance with applied magnetic field (positive magnetoresistance) for $V[TCNE]_x$ at room temperature, up to ~ 0.7% at H = 6 kG. Squeezing of electron wave functions by magnetic field (a mechanism for the positive magnetoresistance in conventional disordered semiconductors) predicts a magnetoresistance three orders of magnitude less than the observed value. We suggest that the initial metallic half-filled π* electronic TCNE band is split by strong Coulomb repulsion into two subbands. Electrons occupying the low subband are coupled antiferromagnetically with the three 3d electrons of V^{II} and as a result the two π* subbands are oppositely spin polarized. The present model explains the observed anomalous value of magnetoresistance and its variations with magnetic field and temperature.

Keywords: Electronic Spin Resonance, Transport Measurements, Magnetotransport, Magnetic films, Magnetic phase transitions, Magnetic devices.

1. Introduction

In the past decade there has been extensive progress in using the spin property of electrons in inorganic multilayers as a means of introducing revolutionary new types of electronics (e.g., spin valves, spin light-emitting diodes) termed spintronics [1]. Challenges including improved spin injection through interfaces, low sensitivity, as well as low Curie temperatures remain [2]. We report that these challenges may be overcome with polymers due to the flexibility of organic chemistry. The conductivity of conjugated polymers is controlled over 15 decades by doping and structural order [3,4]. Similarly bright electroluminescence has been achieved in polymer films [5].

Organic-based magnetism started with discovery [6] in the mid 1980's of ferromagnetism at 4.8 K in the salt $[FeCp^*_2][TCNE]$ ([TCNE] = tetracyanoethylene (Fig. 1, inset(a)); Cp* = pentamethylcyclopendiene). Among the many organic-based magnets since reported, $V[TCNE]_x$ is "soft" ferrimagnet with ordering at T_c ~ 400 K, a small coercive field H_c = 4.5 G at 300 K, and semiconducting conductivity σ_{RT} ~ 10^{-4} S/cm. It can be prepared at 40° C using chemical vapor deposition (CVD) [7].

We propose the concept of spintronics in polymer devices as all the mandatory elements can be achieved with polymers. A key advantage of polymer-based spintronics is the long spin coherence time τ_s. From electron paramagnetic resonance (EPR) data this time is 10^{-7} s for poorly conducting polymers and reaches μs for well conducting samples [8]. Even in the $V[TCNE]_x$ magnet [9] τ_s ~ 10^{-8} s, which is larger than that of typical inorganic semiconductors ~ 10^{-9} s. Another potential advantage of organic structures over inorganic ones is using chemistry to tune the interfaces [10].

Here we present the results of magnetotransport studies [11] of $V[TCNE]_x$ films to evaluate its potential applicability as electron spin aligners. It is critical for spintronic applications to observe that the charge conduction is provided by spin polarized carriers.

2. Magnetotransport Data and Discussion

The samples fabricated as solvent-free CVD prepared thin films were characterized magnetically with electronic paramagnetic resonance (EPR). Figure 1 shows the magnetization (a result of integrating the EPR-signal) of a film vs temperature. Study of the lower Curie temperature T_c sample (T_c ~ 230 K) enables us to probe magnetotransport above and below T_c. Below T_c there is anisotropy in the resonance magnetic field (inset (b), Fig. 1) due to the dependence of the demagnetization factor on the orientation of magnetic field to the film.

0379-6779/03/$ – see front matter
doi:10.1016/S0379-6779(02)00850-0

Figure 2 shows the dc-conductivity as function of temperature for a film of $T_c \sim 280$ K. The conductivity temperature dependence varies little with change in T_c. There is a fit to Mott's 3D variable range hopping (VRH) for localized charge carriers [12] $\sigma_{dc} \sim T^{-1/2} \exp[-(T_0/T)^{1/4}]$ with $T_0 = 2.0\times10^9$ K. Here $k_B T_0 = B/[N(\varepsilon_F)\xi^3]$, where B = 21.2, $N(\varepsilon_F)$ is the density of states at the Fermi level, and ξ is the localization radius. Assuming $\xi \sim 0.5$ nm (size of

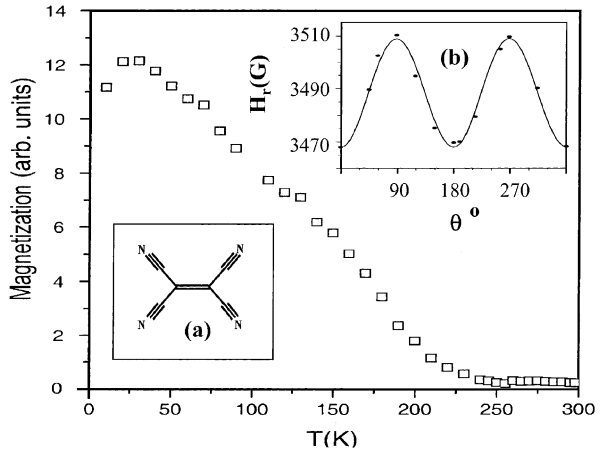

Figure 1. Magnetization (from EPR) of a $V[TCNE]_x$ film *vs* T for H = 3510 G directed perpendicular to a film. Insets: (a) structure of TCNE; (b) anisotropy of EPR resonance field H_r at T = 100 K.

TCNE), we find $N(\varepsilon_F) \sim 1.0\times10^{18}$ $(eV)^{-1}\times cm^{-3}$ too low for the charge density obtained from space filling arguments $n \sim 1/(0.5\text{ nm})^3 \sim 10^{22}$ cm^{-3}. Therefore, we replot the $\sigma(T)$ for a simple activation law with energy gap $\Delta E \sim 0.5$ eV (inset, Fig. 2).

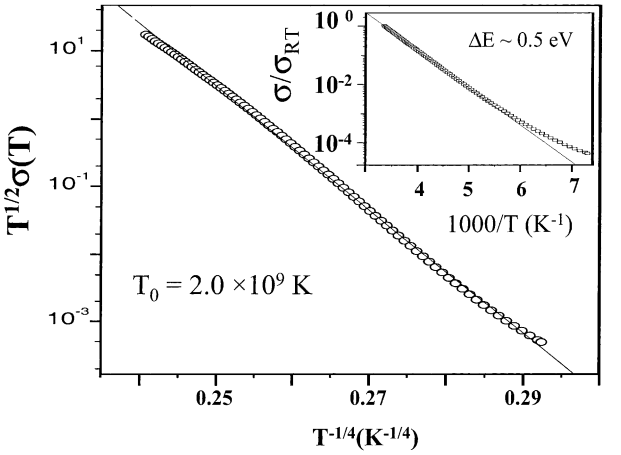

Figure 2. Conductivity of $V[TCNE]_x$ film ($T_c \sim 280$ K) plotted as $T^{1/2}\sigma(T)$ *vs* $T^{-1/4}$ (3D VRH). Inset: fit of $\sigma(T)$ to the activated (Ahrrenius) behavior.

Figure 3 shows the magnetoresistance of $V[TCNE]_x$: $MR = [\rho(H,T)-\rho(0,T)]/\rho(0,T)$ as a function of temperature for a film with $T_c = 235$ K. The applied field H = 6 kG is parallel to the film. The same MR is observed for the magnetic field perpendicular to the film. The maximum of MR(T) is below but close to T_c. The inset in Figure 3 illustrates the H-dependence of MR for T = 215 K and magnetic field parallel to the film. Similar linear field

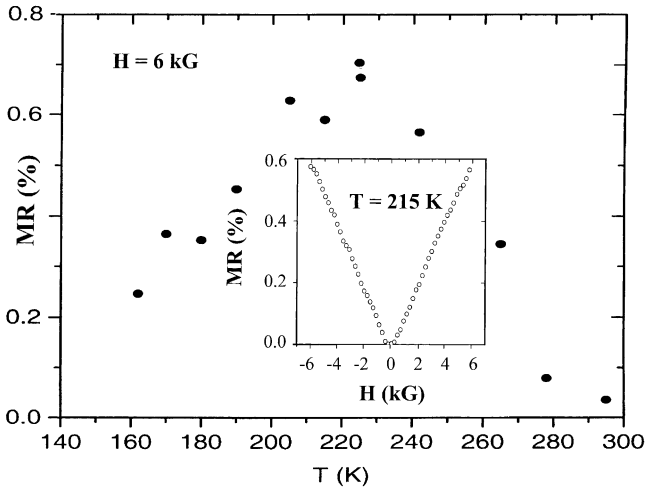

Figure 3. Temperature dependence of magnetoresistance in $V[TCNE]_x$ film for plane of the film parallel to the applied field H = 6 kG for the sample of Fig. 2. Inset: MR(H) for T = 215 K.

dependence was obtained for all temperatures below T_c and samples with different T_c.

The positive magnetoresistance of conventional nonmagnetic semiconductors with $\rho(T) = \rho_0 \exp[(T_0/T)^{1/4}]$ is accounted for a model of squeezing localized wave functions in the presence of magnetic field. For a weak field the theory yields [12]: $\ln[\rho(H,T)/\rho(0,T)] = A(\xi/\lambda)^4(T_0/T)^{3/4}$, where A = 5/2016 and λ is the magnetic length: $\lambda = (c/eH)^{1/2}$. The regime of weak field is valid so long as $\lambda >> \xi$. For $V[TCNE]_x$ the localization length $\xi \sim 0.5$ nm, $\lambda = 33.1$ nm for H = 6 kG, and experimentally $T_0 = 2.0\times10^9$ K. For T = 215 K and H = 6 kG we find $\ln[\rho(H,T)/\rho(0,T)] = 3.6\times10^{-6}$, i.e., the MR is very small $\sim 3.6\times10^{-6}$. We tested this conclusion using sulfonated polyaniline [13] with hopping transport and no MR was detected at these temperatures.

Thus, the observed $MR \sim 6\times10^{-3}$ in $V[TCNE]_x$ is larger than that for conventional semiconductors by three orders of magnitude. Also the experimental field and temperature dependencies of MR are not consistent with the conventional model.

3. Model of a Half – Semiconductor

To explain the anomalous MR we consider the electronic structure and the energy diagram of $V[TCNE]_x$. From average stiochiometry and the magnetic saturation moment it is assumed [14] that the vanadium is in the V^{II} oxidation state and the $TCNE^-$ is the radical anion with its

unpaired electron in the π*-orbital. For V^{II} it is anticipated that the spins of three electrons at 3d level are parallel with total spin of 3/2. In Figure 4 we plot a one-dimensional "cartoon" for the spatial distribution of energy levels in $V[TCNE]_2$. V^{II} is shown alternating with two $[TCNE]^-$ ions to reflect the stiochiometry. The orientation of electronic spins in the π*-state is opposite to the 3/2-spin of V^{II} due to the large antiferromagnetic exchange coupling J.

The charge transport involves hopping among [TCNE]s. The π*-orbital of each [TCNE] can accept two electrons with opposite spins, but the energy of this double occupied $[TCNE]^{2-}$ includes the additional Coulomb repulsion U_c. In analogy with known organic materials and

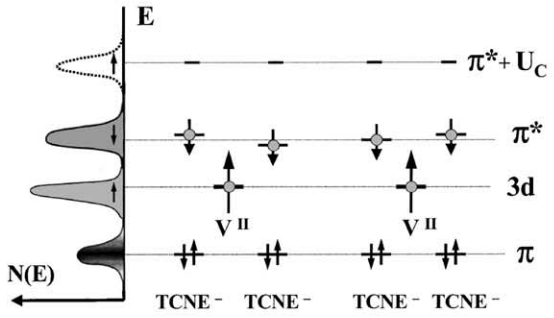

Figure 4. Schematic of level diagram for $V[TCNE]_2$. Half-filled π*-band of $[TCNE]^{\bullet-}$s is split into two non-overlapping Hubbard subbands by the strong Coulomb repulsion U_c.

from the activation energy of conductivity the effective U_c is ~ 0.5 eV. The relevant model for description of electronic states on TCNEs is the Hubbard model with nearly half-filling [15]. Here the π* band is split into two nonoverlapping subbands provided $U_c >> t$, where t is the electronic transfer-integral between neighboring TCNEs.

The spins of electrons in the lower filled Hubbard subband should have antiferromagnetic order but the corresponding exchange constant $J' = 2t^2/U_c$ is much less than the antiferromagnetic exchange constant J between spins of V^{II} and $[TCNE]^-$. Therefore, in the magnetic phase the electronic spins of lower subband are parallel and their orientation is opposite to the spin of V^{II}. According to the Pauli exclusion principle, the upper empty subband may be occupied by electrons with spins polarized in the direction opposite to the lower subband, i.e. along the direction of the V^{II} spins.

For the nearly stiochiometric case the temperature dependence of conductivity is determined by thermal activation across the energy gap. Applying the magnetic field changes the activation gap. Taking into account the opposite spin polarizations of π* subbands and their antiferromagnetic coupling with V^{II} spins, the energy gap ΔE is approximated as $\Delta E = U_c - 4J\langle S\rangle\langle\sigma\rangle$, where $\langle S\rangle$ is the spin 3/2 polarization of V^{II} and $\langle\sigma\rangle$ is the spin 1/2 polarization of lower π* subband.

In the paramagnetic phase the spin polarizations are induced by an external magnetic field and become noticeable only upon approaching T_c. Within the mean field theory [16] $\langle S\rangle \sim -\langle\sigma\rangle \sim \chi h$, where χ is the Curie-Weiss susceptibility per spin, $\chi \sim 1/\delta$, with $\delta = (T - T_c)/T_c$ being the "distance" from T_c ($k_B T_c \sim 3.2$ J). Here $h = \mu_B gH/(k_B T_c) << 1$ and $h^{2/3} << \delta << 1$. As a result the gap widens with the applied field and MR ~ $(h/\delta)^2$.

In the critical region, $|\delta| << h^{2/3}$, the induced polarization obeys the scaling law $\langle S\rangle \sim -\langle\sigma\rangle \sim h^{1/3}$ and MR ~ $h^{2/3}$. Below T_c ($|\delta| >> h^{2/3}$, $\delta < 0$), there is the spontaneous spin polarization $\langle S\rangle \sim -\langle\sigma\rangle \sim |\delta|^{1/2}$ with field dependent corrections ~ χh, where $\chi \sim 1/|\delta|$. Therefore, in the ferrimagnetic phase the MR is proportional to a magnetic field, MR ~ $h/|\delta|^{1/2}$.

As a function of temperature, the MR has its maximum near T_c. For H = 6 kG and T_c = 230 K the model predicts the MR maximum ~ $h^{2/3}$ ~ 2%, which is of the order of the observed value.

4. Conclusions

Thus, the experimental results for resistance and MR of organic-based magnet $V[TCNE]_x$ support the existence of spin polarized subbands – a half semiconducting state - in which the electron spins in "valence and conduction bands" are oppositely polarized. This is a very desirable property for utilizing organic-based magnetic semiconductors in spintronic applications.

References

† Supported in part by DARPA (N00014-02-1-0593), ARO (DAAD19-01-1-0562), and DOE (DE-FG02-01ER45931).
* Corresponding author. Email: epstein.2@osu.edu
[1] S.A. Wolf, J. Supercond. 13 (2000) 195.
[2] H. Ohno, J. Magn. Magn. Mater 242 (2002) 105.
[3] V.N. Prigodin and A.J. Epstein, Synth. Met. 125 (2002) 43.
[4] R.S. Kohlman and A.J. Epstein, in *Handbook of Conducting Polymers*, edited by T.A. Skotheim, R.L. Elsenbaumer, and J.R. Reynolds, Marcel Dekker, Inc., New York, 1998, p. 85.
[5] Y.Z. Wang and A.J. Epstein, Acct. Chem. Res. 32 (1999) 217.
[6] J.S. Miller, J.C. Calabrese, A.J. Epstein, R.W. Bigelow, J.H. Zhang, W.M. Reiff, J. Chem. Soc., Chem. Commun. (1986) 1026; S. Chitteppeddi, K.R. Cromack, J.S. Miller, and A.J. Epstein, Phys. Rev. Lett. 58 (1987) 2695.
[7] K.I. Pokhodnya, A.J. Epstein, and J.S. Miller, Adv. Mat. 12 (2000) 410.
[8] J. Joo, S.M. Long, J.P. Poget, E.J. Oh, A.G. MacDiarmid, and A.J. Epstein, Phys. Rev. B 57 (1998) 9567.
[9] S.M. Long, P Zhou, J.S. Miller, and A.J. Epstein, Mol. Cryst. Liq. Cryst. 272 (1995) 207.
[10] N.C. Greenham and R.H. Friend, *Semiconductor Device Physics of Conjugated Polymers*, Academic Press, Inc., San Diego, 1999.
[11] V.N. Prigodin, N.P. Raju, K.I. Pokhodnya, J.S. Miller, and A.J. Epstein, Adv. Mater. 14 (2002) 1230.
[12] B.I. Shklovskii and A.L. Efros, *Electronic Properties of Doped Semiconductors*, Springer-Verlag, Berlin, 1984, 155.
[13] W.P. Lee, K.R. Breneman, A.D. Gudmundsdottir, M.S. Platz, P.K. Kahol, A.P. Monkman, and A.J. Epstein, Synth. Met. 101 (1999) 819.
[14] J.S. Miller and A.J. Epstein, J. Chem. Soc., Chem. Commun. (1998) 1319.
[15] S. Onoda and M. Imada, J. Phys. Soc. Jpn. 70 (2001) 3398.
[16] J.M. Yeomans, *Statistical Mechanics of Phase Transitions*, Oxford Univ. Press, N.Y., 1992, 128.